Published online July 7, 2004

3590–3600 *Nucleic Acids Research, 2004, Vol. 32, No. 12*
doi:10.1093/nar/gkh687

The 'scavenger' m^{7}GpppX pyrophosphatase activity of Dcs1 modulates nutrient-induced responses in yeast

Naglis Malys, Kathleen Carroll, Jaleel Miyan, David Tollervey[1] and John E. G. McCarthy*

Posttranscriptional Control Group, Department of Biomolecular Sciences, University of Manchester Institute of Science and Technology (UMIST), Manchester M60 1QD, UK and [1]Wellcome Trust Centre for Cell Biology, University of Edinburgh, Michael Swann Building, King's Buildings, Mayfield Road, Edinburgh EH9 3JR, UK

Received May 6, 2004; Revised and Accepted June 17, 2004

ABSTRACT

Dcs1, the m^{7}GpppX pyrophosphatase of *Saccharomyces cerevisiae*, has been reported to 'scavenge' capped 5′ end fragments generated by 3′→5′ mRNA degradation. We now show that the absence of Dcs1, and the closely related Dcs2 protein, compromises cellular responses to glucose-deprivation stress as well as to step changes in glucose availability. Dcs1 and Dcs2 form homo- and heterodimers, with the heterodimer appearing as cells enter diauxie. Despite the previously observed increase in abundance of the mRNA encoding the neutral trehalase (Nth1) in the stationary phase, the total enzyme activity of Nth1 decreases in this phase of growth. Changes in trehalase activity are significant because the non-reducing disaccharide trehalose is thought to stabilize cellular components under stress conditions. In the *dcs1*Δ and *dcs1*Δ*dcs2*Δ mutants, normal regulation of trehalase activity is lost. Nutrient stress induces *DCS1* and *DCS2* transcription via the cAMP-PKA signalling pathway. Dcs1 also becomes phosphorylated as the availability of glucose diminishes, and we test the role of this phosphorylation in the stress response. Further evidence indicates that Dcs1 plays a complementary role to the translation factor eIF4E in preventing capped 5′ fragments of mRNA from interfering with translation initiation. We conclude that Dcs1 function influences cellular responses to changes in nutrient avialability, while Dcs2 seems to act as a modulator of Dcs1 function.

INTRODUCTION

In living cells, enzyme-catalysed degradation processes determine the lifetimes of different mRNAs and thereby influence their steady-state levels. mRNA decay therefore plays an important role in the post-transcriptional control of gene expression (1). The degradation of eukaryotic mRNA is performed largely by exonucleases, whereby access of these enzymes to the body of the mRNA requires removal of either the 3′ poly(A) tail, the 5′ cap, or of both (2–4). Decapping is an important rate-controlling step, since it exposes the 5′ end of mRNAs to attack by 5′→3′ exonucleases of the Xrn1 type (5). Work in the yeast *Saccharomyces cerevisiae* has identified two proteins, Dcp1 and Dcp2, as involved in m^{7}GDP-generating decapping, and homologues of these proteins exist in higher eukaryotes (6,7). However, an m^{7}GMP-generating decapping activity detected in mammalian cells has been identified [DcpS (2,8)], and related enzymes have been partially characterized in both *S.cerevisiae* [Dcs1 and Dcs2 (9)] and in *Schizosaccharomyces pombe* [Nhm1 (10)]. It has been proposed that the Dcs-type proteins act as 'scavenging' pyrophosphatases that help mop up short, capped mRNA fragments left over from 3′→5′ exonucleolytic decay (2,8).

Little is known about modulation of mRNA decay pathways under conditions of stress. In general, *S.cerevisiae* regulates gene expression in response to nutrient, temperature and osmotic stresses. This generally involves coordinate transcriptional regulation of different groups of genes. *S.cerevisiae* has both stress-specific stress factors and more general stress factors. Msn2 and Msn4 are two related factors of the latter type. They become active both during the diauxic shift and under a broad range of stress conditions (11,12). These factors may generally receive and integrate signals from different stress-signalling pathways. They bind to DNA *cis*-acting stress response elements (STREs) that control a large number of genes. Glucose and cAMP down-regulate *MSN2/4* and consequently the STRE-controlled genes (13). Thus, Msn2/4 factors are implicated in PKA-dependent regulation of STRE-controlled gene expression (11,12,14). The Rim15 protein kinase is identified as a downstream target of PKA that acts as an activator of STRE-controlled gene expression (14). The cAMP-PKA pathway is also connected to the nutrient-regulated protein kinases Sch9 and Yak1/Sok1 (14). Protein kinases Rim15 and Yak1 are required for proper cell entry into the stationary phase and suppress the growth arrest caused by PKA depletion, as does deletion of *MSN2/4* (15). Recently, Yak1, along with phosphoprotein Pop2, were proposed to function as part of a novel glucose-sensing system in yeast that is involved in growth control in response to glucose availability (16).

The cAMP-PKA pathway is linked to a complex network of signalling cascades. Other components of this network,

*To whom correspondence should be addressed. Tel: +44 161 200 8916; Fax: +44 161 200 8918; Email: j.mccarthy@umist.ac.uk

including the TOR (*t*arget *o*f *r*apamycin), PKC MAPK (protein kinase C *m*itogen-*a*ctivated protein *k*inase) and HOG (*h*igh-*o*smolarity *g*lycerol) MAPK pathways, also regulate gene expression in response to stress conditions (17–19). Recently, it was revealed that activation of the cAMP-PKA pathway suppresses TOR deficiency (20). Moreover, TOR can regulate PKA through control of the subcellular localization of both the PKA catalytic subunit Tpk1 and the kinase Yak1 (20). Other results suggest that the HOG pathway may regulate Msn2/4, possibly via cAMP/PKA (18).

In this paper, we characterize how nutrient stress influences the expression of yeast *DCS1* and *DCS2* at the transcriptional and post-transcriptional levels. Dcs1 function compromises the nutrient stress response and apparently leads to de-regulated synthesis of the stress-response disaccharide, trehalose. We discuss possible mechanisms underlying these regulatory phenomena and the basis for functional interactions between Dcs1 and the cap-binding complex eIF4F.

MATERIALS AND METHODS

Yeast growth conditions

Yeast strains were as shown in Table 1. Cells were grown in liquid YPD (1% yeast extract, 2% peptone, 2% glucose) and in minimal YNB medium (0.67% yeast nitrogen base, 2% glucose) supplemented with uracil and selected amino acids, or on plates containing YPD plus 2% agar. For growth under different conditions, cultures of exponentially growing cells were divided into smaller volumes, washed and resuspended in liquid media containing different carbon sources (glucose, glycerol, trehalose). Alternatively, cultures were serially diluted on YPD, YP, YP(gal), YP(glyc), YPD(H_2O_2) and YPD(NaCl) agar plates.

Table 1. Strains used in this work

Strain	Genotype	Source
BY4741	*MAT*a *his3Δ1 leu2Δ0 met15Δ0 ura3Δ0*	EUROSCARF
BY4742	*MAT*α *his3Δ1 leu2Δ0 lys2Δ0 ura3Δ0*	EUROSCARF
PTC194	*MAT*a *his3Δ1 leu2Δ0 met15Δ0 ura3Δ0 dcs1*::*LEU2*	This study
Y12429	*MAT*α *his3Δ1 leu2Δ0 lys2Δ0 ura3Δ0 dcs2*::*kanMX4*	EUROSCARF
PTC195	*MAT*a *his3Δ1 leu2Δ0 met15Δ0 lys2Δ0 ura3Δ0 dcs1*::*kanMX4 dcs2*::*kanMX4*	This study
PTC196	*MAT*α *DCS1-TAP-URA3 his3Δ1 leu2Δ0 lys2Δ0 ura3Δ0*	This study
PTC197	*MAT*α *DCS2-TAP-URA3 his3Δ1 leu2Δ0 lys2Δ0 ura3Δ0*	This study
Y12429H	*MAT*α *his3Δ1 leu2Δ0 lys2Δ0 ura3Δ0 dcs2*::*kanMX4 pURAGAL1-DCS2-HA*	This study
Y12429M	*MAT*α *his3Δ1 leu2Δ0 lys2Δ0 ura3Δ0 dcs2*::*kanMX4 pURAGAL1-DCS2-MH*	This study
PTC194H	*MAT*a *his3Δ1 leu2Δ0 met15Δ0 ura3Δ0 dcs1*::*LEU2 pURAGAL1-DCS1-HA*	This study
PTC194M	*MAT*a *his3Δ1 leu2Δ0 met15Δ0 ura3Δ0 dcs1*::*LEU2 pURAGAL1-DCS1-HA*	This study
MY1	*MAT*a *ura3-52 trp1 leu2*::*PET56 gcn4 gal2*	(15)
MY2677	*MAT*a *ura3-52 trp1 leu2*::*PET56 gcn4 gal2 msn4*::*TRP1 msn2*::*HIS3 ura3*::*STRE-lacZ-URA3*	(15)
MY2872	*MAT*a *ura3-52 trp1 leu2*::*PET56 gcn4 gal2 rim15*::*kanMX*	(15)
MY3273	*MAT*a *ura3-52 his3 trp1 leu2 ade8 tpk1*::*URA3 tpk2*::*HIS3 tpk3*::*TRP1 rim15*::*kanMX yak1*::*LEU2*	(15)
MY3297	*MAT*a *ura3-52 trp1 leu2*::*PET56 gcn4 gal2 rim15*::*kanMX yak1*::*LEU2*	(15)
YTH3	*MAT*a *his3Δ1 leu2Δ0 met15Δ0 ura3Δ0 CDC33(−198, −1)*::*KanMX4-tTA-tetO7*	(40)
YTH3 dcs1Δ	*MAT*a *his3Δ1 leu2Δ0 met15Δ0 lys2Δ0 ura3Δ0 dcs1*::*kanMX4 CDC33(−198, −1)*::*KanMX4-tTA-tetO7*	This study

Plasmids

PCR fragments bearing the *DCS1* and *DCS2* ORFs plus flanking sequences were digested with XbaI and Bsp120I and cloned into pRS313 and pRS315 (21), yielding pRS313-*DCS1* and pRS315-*DCS2*, respectively. These plasmids were used for complementation analyses of *dcs1*Δ and *dcs2*Δ strains. Plasmids pRS313-*DCS1*-178 (S60A) and pRS313-*DCS1*-196 (T66A) were constructed after PCR-mediated site-directed mutagenesis [performed according to (22)]. Plasmids p*URAGAL1-DCS1*-HA, p*URAGAL1-DCS1*-MH, p*URAGAL1-DCS2*-HA and p*URAGAL1-DCS2*-MH were constructed using YCpSUPEX2 (23) by inserting genes *DCS1* and *DCS2* tagged with either haemagglutinin or Myc epitope. To construct a plasmid for recombinant Dcs1 protein expression, an NdeI–XbaI fragment encoding His8-tagged Dcs1 protein was PCR-amplified from *S.cerevisiae* genomic DNA and inserted into the pET5A vector (Novagen), yielding pET5A-*DCS1*. Plasmid pBS1539 (24) was used as the PCR template in the generation of TAP fusion strains PTC196 and PTC197.

Protein purification and sequencing

Dcs2 protein was purified both as the TAP fusion version, and as the non-tagged protein using a two-step purification technique procedure (24). Dcs2–TAP fusion protein was co-purified with the Dcs1 protein. Non-tagged Dcs2 protein was purified as part of the Dcs1–Dcs2 complex isolated via the Dcs1–TAP fusion protein. Of each purified protein complex, 1–2 μg was precipitated using 10% trichloroacetic acid and fractionated on a 10% SDS–PAGE gel. The proteins were electro-transferred to a PVDF membrane and visualized by staining in 0.25% Coomassie Blue R-250, 40% methanol, 1% acetic acid for 1–2 min, followed by destaining in several changes of 40% methanol for 5–10 min. Dcs2–TAP and Dcs2 proteins were excised and used in N-terminal sequence determination (peptide sequencing at the University of Liverpool). Recombinant His-tagged Dcs1 protein [generated from pET5A-DCS1 plasmid in *Escherichia coli* BL21(DE3) CodonPlus RIL cells] was purified using a nickel affinity column (Novagen) followed by a Resource Q column (Amersham).

Mass spectrometry

Sinapinic acid and calibration standards for mass spectrometry were obtained from Sigma. The MALDI matrix was 10 mg/ml sinapinic acid in 50% acetonitrile–aqueous 0.05% trifluoroacetic acid (TFA). BSA at a concentration of 10 pM (66.4 kDa) and 2 pM apomyoglobin (16.9 kDa) were used as calibrants,

mixed and applied in a 1:1 ratio with the matrix. The sample (Dcs1–TAP and Dcs2 in water) was mixed 1:1 with the matrix and applied to a stainless steel MALDI target and left to dry at room temperature. Positive ion linear MALDI-TOF MS spectra were acquired on an AXIMA-CFR (Kratos Analytical, Shimadzu Biotech, UK).

Fluorescence microscopy

Cells were grown in YPD to mid-log phase, fixed by incubation in 4% (v/v) formaldehyde for 30 min at 30°C, and converted to spheroplasts. The TAP fusion was detected using a rabbit anti-protein A antibody (diluted 1:200, Sigma) and a secondary FITC-conjugated goat anti-rabbit IgG (1:100, Vector laboratories, Inc). Haemagglutinin and Myc epitope-tagged proteins were allowed to react, respectively, with rabbit polyclonal anti-haemagglutinin antibodies (1:100, Sigma) followed by FITC-conjugated goat anti-rabbit IgGs (1:100), and with a mouse monoclonal anti-c-Myc antibody (1:50, Sigma) followed by Texas red-conjugated horse anti-mouse IgG (1:100, Vector laboratories, Inc). Nuclear DNA was stained with 4′,6-diamidino-2-phenylindole (DAPI) that was included in the mounting medium (Vector Laboratories, Inc). Cells were analysed using a confocal microscope (Zeiss LSM510; objective: HC Plan APO OS 100× oil NA 1.4).

Western blotting

Crude extracts were prepared from cultures using glass beads. Equal amounts of protein were separated via SDS–PAGE and transferred to a PVDF membrane (Amersham). Rabbit anti-Dcs1 antibodies were prepared (CovalAb UK Ltd) against recombinant Dcs1–His_8 protein generated in *E.coli*. Dcs2 was detected in the form of Dcs2–TAP using PAP antibodies (Sigma). Immunoreactions on the membrane were visualized by chemiluminescence (ECL, Amersham).

RNA extraction, northern hybridization and primer extension analysis

RNA was extracted from cells at the stated time points and northern blots were performed as described elsewhere (25). Primer extension analysis was performed using AMV reverse transcriptase (Promega) and the ^{32}P-labelled oligonucleotide 5′-GGTTCGAATCTAACACCCTGACG.

Assay of trehalase activity and glucose measurement

Nth1 activity was estimated using the glucose oxidase/peroxidase method (GAGO-20 kit, Sigma). The assay was performed using crude extracts as described previously (26).

[32P]orthophosphate labelling and immunoprecipitation

The *S.cerevisiae* strains BY4741 and PTC194 were grown to OD_{600} = 0.2 in reduced phosphate medium that was prepared by adding KH_2PO_4 to phosphate-free medium (27) to a final concentration of 1 mM. Cells were pelleted from 10 ml samples of the strains, and resuspended in the same volume of either phosphate-free medium with glucose, or in phosphate-free medium without glucose. Cells were grown to OD_{600} = 0.8. Then 250 µCi of [^{32}P]orthophosphate (Amersham) were added to each sample and the cells were allowed to grow for another 45 min. The cells were then pelleted again and frozen. Each pellet was resuspended in 200 µl of buffer IP [50 mM Tris–HCl, pH 7.5, 150 mM NaCl, 0.1% NP-40, 0.5 mM PMSF, protease inhibitor cocktail (Sigma)] at 4°C. The cells were lysed with glass beads and each supernatant was incubated with 15 µl of anti-Dcs1 antibodies for 2 h at 4°C. Then 20 µl of Protein-A Sepharose™ CL-4B (Amersham) equilibrated in IP buffer was added to each sample, followed by incubation for 2 h at 4°C. The immunoprecipitates were washed 8 times with 1 ml of buffer IP. A 50 µl aliquot of SDS loading buffer was added and the samples were denatured at 95°C for 5 min. The supernatant of each sample was divided and analysed on two 10% SDS–PAGE gels, which were used for western blotting and autoradiography, respectively.

RESULTS

DCS1 and *DCS2* expression signals

Examination of the *DCS1* (*YLR270w*) DNA sequence reveals the presence of a single open reading frame with a predicted product (M_r = 40.6 kDa) that corresponds to the electrophoretic migration behaviour of Dcs1 (as detected by western blotting in yeast—see below). No known regulatory motifs are evident in the proximity of the *DCS1* promoter region. In contrast, comparison of the DNA sequence of *DCS2* (*YOR173w*) with the previously estimated size of the encoded protein does not allow unequivocal identification of this gene's reading frame. We therefore determined the transcriptional and translational start sites of *DCS2*. The 5′ end of the *DCS2* mRNA was characterized by means of primer extension (Figure 1A). Examination of the sequences upstream of this transcriptional start site revealed the presence of stress-response elements [STREs (12,28)] in the *DCS2* DNA sequence (Figure 1B). N-terminal protein sequencing also defined the correct position of the translation start codon, revealing that Dcs2 is 352 amino acids long (M_r = 39.9 kDa). This makes Dcs2 45 amino acids shorter than the protein that would be predicted using the ATG previously assumed to be the start codon (NCBI database, see upstream ATG highlighted in Figure 1B).

Dimerization and subcellular localization of the Dcs proteins

In order to identify complexes formed by the Dcs proteins, we used the TAP procedure (24) to pull down potential binding partners from cell lysates. Using either Dcs1-TAP or Dcs2-TAP, we observed the formation of both homo- and heterodimers (Figure 1C and D). The MALDI spectrum (Figure 1D) does not resolve the two CBD-tagged Dcs1 species evident in SDS–PAGE, which are evidently very similar in terms of molecular mass (Figure 1C; see also Figure 4). These data are consistent with the previous observations (2,8,29) that the related human $m^7G(5')$pppN-pyrophosphatase, which has a similar monomeric size, has an apparent M_r of ~80 kDa as determined by sedimentation analysis and gel filtration.

We assessed the subcellular distribution of Dcs1 and Dcs2 using fusions carrying protein A, haemagglutinin or c-Myc tags. Fluorescence microscopy performed using Dcs1 and Dcs2 tagged with protein A revealed that both proteins are predominantly cytoplasmic (Figure 2), and thus present in the same compartment in which the degradation of mature mRNAs and the metabolism of carbohydrates takes place.

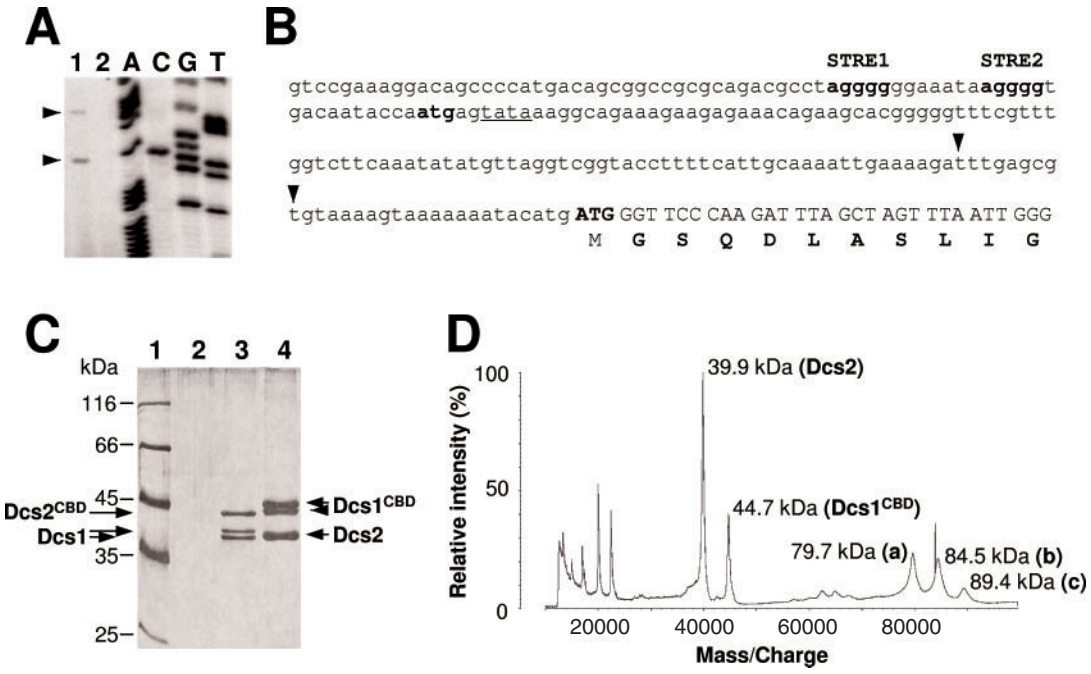

Figure 1. Characterization of *DCS2* mRNA 5′ ends and Dcs1/Dcs2 dimeric complexes. (**A**) Primer extension analysis was performed on *DCS2* mRNA using total RNA isolated from *S.cerevisiae* BY4741 cells at mid-log phase (lane 1). In the control, total RNA was treated with RNase A before the primer extension reaction (lane 2). Each sequencing lane is labelled with the dideoxynucleotide used in the sequencing reaction. (**B**) Sequence of the upstream region of the *DCS2* gene. The correct initiation codon leads off the N-terminal sequence confirmed by amino acid sequencing. The ATG upstream of this, which was originally thought to be the start codon of *DCS2*, is also shown in bold type. Potential STRE elements are in bold, while a typical promoter TATA motif is underlined. Arrowheads indicate the 5′ ends detected by the primer extension analysis. (**C**) A silver-stained, 10% SDS–PAGE gel shows the proteins found in the complexes purified using Dcs1–TAP and Dcs2–TAP. Lane 1, molecular mass markers (kDa); lane 2, TAP purification from strain BY4741, as negative control; lane 3, TAP purification from strain PTC197 (Dcs2–TAP); lane 4, TAP purification from strain PTC196 (Dcs1–TAP). The identities (confirmed by MALDI) of the respective proteins running in lanes 3 and 4 are indicated by labelling on the sides of the gel. Two forms of both Dcs1 and Dcs1^{CBD} are evident (compare Figure 5A and B). CBD (calmodulin binding domain) indicates proteins that still carry part of the TAP tag. (**D**) Positive ion MALDI mass spectrum of the sample that was analysed in lane 4 of (**C**) The spectrum reveals the presence of Dcs1^{CBD} and Dcs2 monomers, of homodimers of Dcs2 (a) and Dcs1^{CBD} (c), as well as of the Dcs2–Dcs1^{CBD} heterodimer (b). M_r values are indicated next to the corresponding peaks.

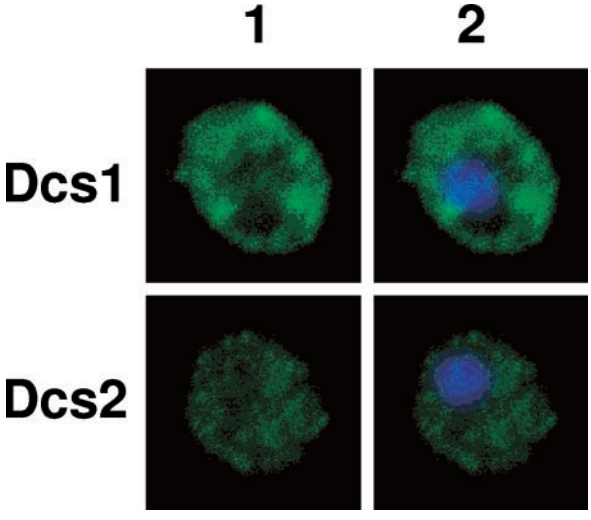

Figure 2. Subcellular localization of Dcs1 and Dcs2 proteins in *S.cerevisiae* cells. Strains expressing Dcs1–TAP and Dcs2–TAP were examined by indirect immunofluorescence microscopy using the antiserum directed against protein A and FITC-conjugated anti-rabbit secondary antibodies (column 1). Nuclear DNA was stained with DAPI in the overlay images (column 2).

Very similar distributions were seen with the HA- and c-Myc-tagged derivatives (data not shown), thus confirming the cytoplasmic location of both proteins. These data are consistent with the previous result of human cell fractionation where the majority of the pyrophosphatase activity was found in the cytoplasmic extract, while ~6% of the total activity was present in the nuclear fraction (8).

Dcs proteins support the cellular response to nutrient stress

We explored the potential role of Dcs proteins in the cellular response to nutrient starvation using disruption mutants constructed using a PCR strategy (30). Glucose is the preferred carbon source for budding yeast, which has an elaborate network of molecular systems for sensing changes in glucose availability and adjusting gene expression and cellular metabolism in response to such changes (31). We observed that the ability of yeast cells to respond to glucose deprivation is compromised when *DCS1* is disrupted, and that this phenotype is exacerbated in the *dcs1*Δ*dcs2*Δ double disruption (Figure 3A). The growth of the *dcs2*Δ strain was difficult to distinguish from that of the wild-type strain, and it is therefore uncertain whether this single disruption has a phenotype. Similar

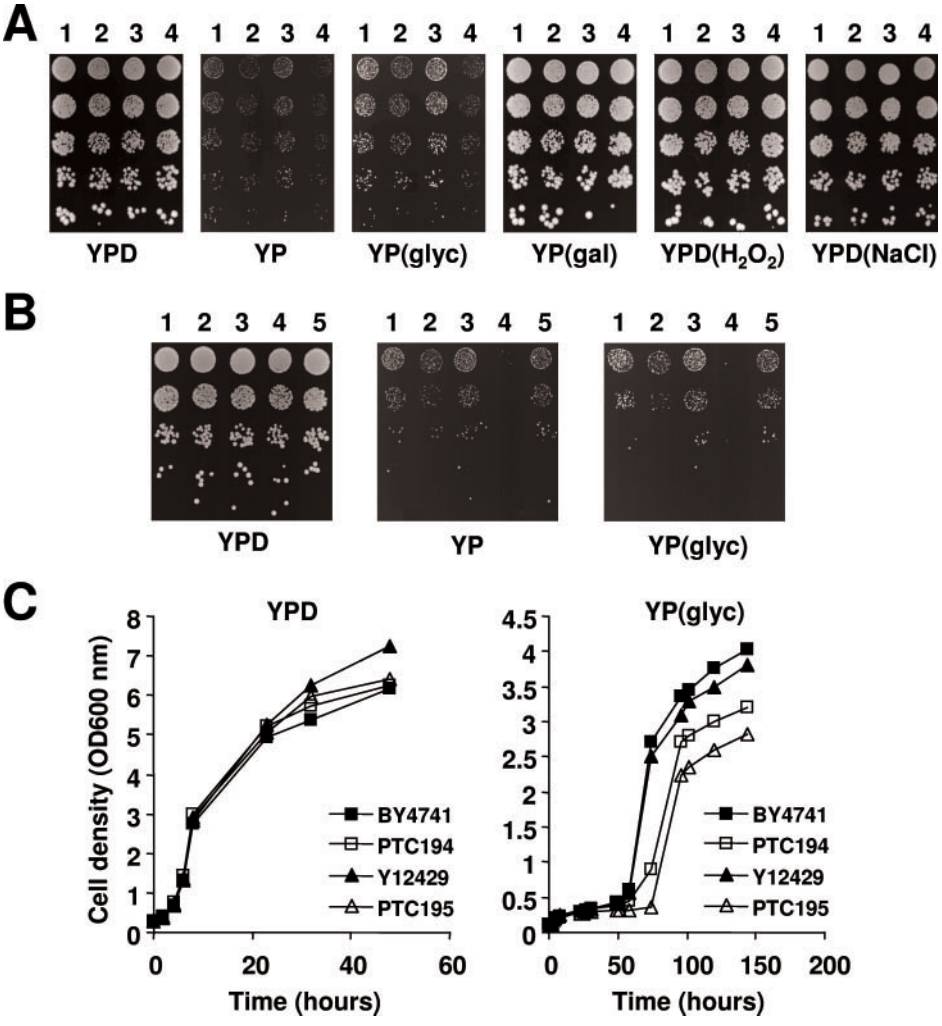

Figure 3. Growth phenotypes of the *dcs* deletion strains on different media. (**A**) The following strains were allowed to reach exponential phase growth in liquid YPD medium, were serially diluted, and then spotted on YPD, YP(gal), YPD(H_2O_2) and YPD(NaCl) agar plates (2 days incubation at 30°C), or YP and YP(glyc) agar plates (6 days incubation at 30°C): BY4741 (lane 1), PTC194 (lane 2), Y12429 (lane 3) and PTC195 (lane 4). (**B**) Cells were grown to mid log phase on minimal YNB medium, serially diluted, and spotted onto YPD agar plates (2 days incubation at 30°C), or onto YP and YP(glyc) agar plates (6 days incubation at 30°C): BY4741 (lane 1), PTC194 (lane 2), PTC194 transformed with pRS313-*DCS1* (lane 3), PTC195 (lane 4), and PTC195 transformed with pRS313-*DCS1* and pRS315-*DCS2* (lane 5). (**C**) Cells of BY4741 (filled squares), PTC194 (open squares), Y12429 (filled triangles) and PTC195 (open triangles) growing exponentially in YPD were washed and transferred to YPD medium and YP(glyc) medium, respectively, and the OD was measured at the indicated time points.

phenotypes for the respective strains were observed when glucose was replaced by glycerol, whereas the availability of galactose significantly reduced the impact of the disruptions. The *DCS* genes were found not to influence growth under conditions of oxidative or osmotic stress in this assay (Figure 3A).

We next tested whether the *DCS* mutations affect the adaptation of yeast to changes in the composition of the growth medium. Both the spot assays on agar plates (Figure 3B) and growth experiments in liquid media (Figure 3C) revealed marked reductions in the ability of yeast to adapt to a shift from minimal medium to YP medium or to YP medium containing glycerol. In control experiments, we found that the growth phenotypes could be suppressed by transformation of the mutant strains with the appropriate *DCS1/2* expression plasmids (Figure 3B, lanes 3 and 5). Overall, we conclude from these experiments that both the nutrient stress response and the nutrient adaptation response in yeast are influenced by the *DCS* genes.

Regulation of *DCS* genes

We next investigated how changes in the available carbon source affect expression of the respective genes. Northern and western blotting were used to compare the levels of mRNA and protein, respectively, encoded by the *DCS* genes in the presence and absence of glucose (Figure 4A). Removal of glucose from YPD medium switched on the synthesis of both *DCS2* mRNA and Dcs2 protein. The observed increase in the mRNA signal correlates with the results of an earlier microarray study of glucose-related changes in the yeast transcriptome (32). *DCS2* was also identified in a screen for cAMP-repressed genes whose expression responds to nutrient limitation (33). Induction of the synthesis of *DCS2* mRNA and Dcs2 protein were also observed under conditions of osmotic, oxidative and heat stress, while cycloheximide treatment induced only *DCS2* mRNA synthesis (data not shown). These results are consistent with the presence of

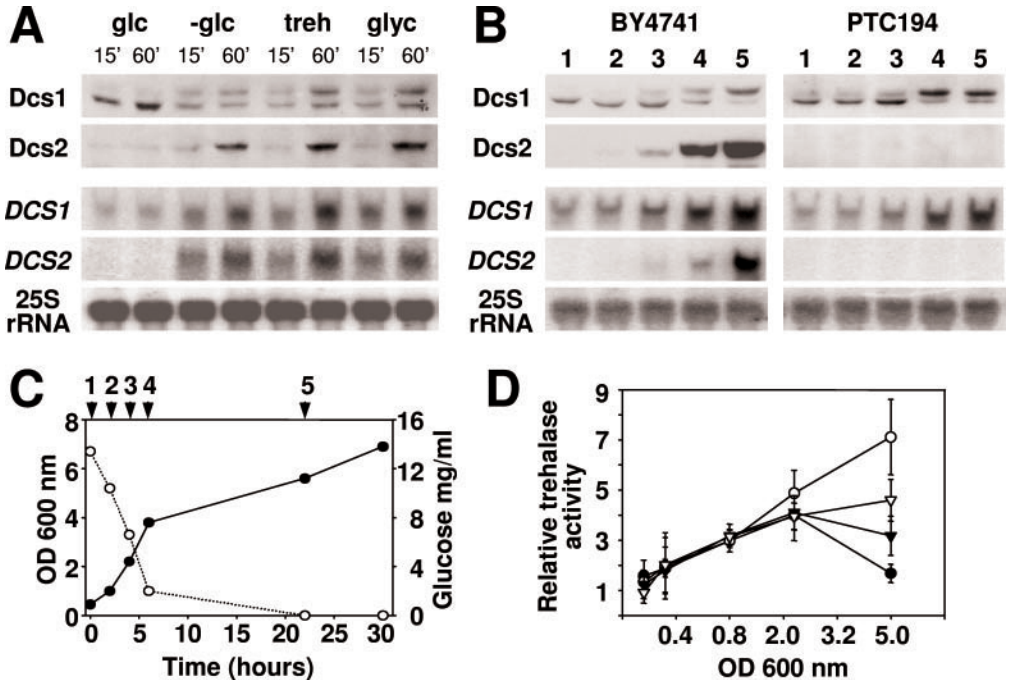

Figure 4. *DCS1* and *DCS2* mRNAs and proteins during diauxic shift and under carbon-source stress conditions. (**A**) Top two rows: western blots using antibodies against Dcs1 and Dcs2, respectively. Dcs2 was detected in the form of Dcs2–TAP using PAP antibodies (Sigma). Bottom two rows: northern blotting was performed using probes against *DCS1* mRNA, *DCS2* mRNA and 25S rRNA, respectively. The cell extracts used in the above were prepared from the wild-type strain BY4741 under the following conditions: glucose depletion, glucose replacement by trehalose and glucose replacement by glycerol. Samples were taken 15 and 60 min, respectively, after the change in carbon source (as indicated). (**B**) Western blotting and northern blotting were performed on cell extracts prepared from the wild-type strain BY4741 and the *dcs2*Δ mutant Y12429 strain. The signals obtained using a probe against 25S rRNA serve as references for the amount of total RNA in each sample. The numbers at the top of each column correspond to the time points indicated in (C). (**C**) The samples used in (B) were taken from this culture of BY4741 at the points indicated. Cell density (filled circles) and glucose concentration (open circles) were measured on all samples. Growth was at 30°C in YPD medium. (**D**) Trehalase activity was measured using the glucose oxidase/peroxidase method (26) in extracts from the wild-type strain (BY4741, filled circles), the *dcs1*Δ strain (PTC194, open circles), the *dcs2*Δ strain (Y12429, closed triangles) and the *dcs1*Δ*dcs2*Δ strain (PTC195, open triangles) at different stages of growth. The increase in trehalase activity is expressed as a ratio to the activity of control cells ($OD_{600} = 0.4$), normalized to 1. The presented data represent averages of three independent experiments.

STRE motifs upstream of the *DCS2* transcriptional start site (Figure 1B), since STREs mediate activation of transcription in response to stress conditions. In the case of *DCS1*, glucose depletion resulted in weaker enhancement of mRNA levels while causing the appearance of a modified form of the Dcs1 protein that ran as a reduced mobility band on SDS–PAGE (Figure 4A and B). The addition of the alternative carbon sources trehalose and glycerol to culture medium lacking glucose exerted only a minor influence on this pattern of expression. Similar increases in the relative *DCS1* mRNA level were observed under osmotic, oxidative, heat stress and metabolic stress conditions. Moreover, a modified form of the Dcs1 protein appeared under all stress conditions, except for cycloheximide treatment (data not shown).

In standard batch culture, glucose depletion occurs during the diauxic shift. Analysis of cells progressing through the logarithmic growth phase to the stationary phase revealed the same transcriptional up-regulation of *DCS2* and post-translational modification of Dcs1 (Figure 4B and C). The critical threshold below which changes in gene expression or protein modification are detectable is ~10 mg/ml glucose which, in this batch culture system, corresponds to $OD_{600} = 0.8$.

A comprehensive two-hybrid analysis of yeast gene products recently revealed that Dcs1 interacts physically with the neutral trehalase, Nth1 (34,35). The latter enzyme is known to control trehalose hydrolysis in response to stress conditions (36,37). Trehalose, which comprises two glucose molecules connected via an α,α−1,1 linkage is accumulated by yeast cells to protect cellular components under various stress conditions (38). Trehalase-catalysed hydrolysis of this disaccharide is activated during recovery from stress, while it is normally repressed in stationary phase (37). We were therefore interested to know whether the stress phenotypes of the respective *dcs*Δ strains might be linked to changes in Nth1 activity, and proceeded to measure trehalase activity in extracts from cell cultures at different times prior and subsequent to the diauxic shift (Figure 4D). We discovered that the *dcs1*Δ strain we had constructed had lost the ability to down-regulate trehalase activity in the stationary phase. The *dcs1*Δ*dcs2*Δ strain had also lost the ability to down-regulate trehalase activity, but manifested somewhat lower levels than the *dcs1*Δ strain. Comparison with the *dcs2*Δ and *dcs1*Δ*dcs2*Δ strains indicates that Dcs2 may play a secondary role to Dcs1 in promoting normal regulation of trehalase. A similar observation of reduced control over trehalase activity was also made recently by de Mesquita *et al*. (39) using a *dcs1*Δ mutant.

Dcs1 is a phosphoprotein

We suspected that the modification of Dcs1 might be phosphorylation, and performed experiments intended to test this hypothesis. *In vivo* labelling using $^{32}P_i$ suggested that the

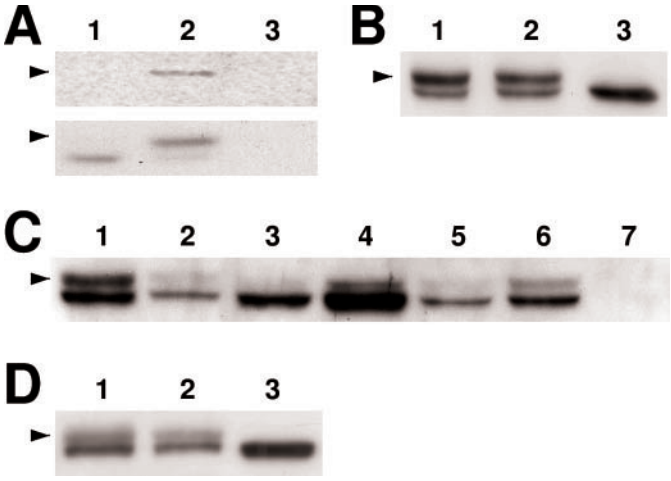

Figure 5. Dcs1 is phosphorylated in response to glucose depletion. (**A**) A [^{32}P]orthophosphate metabolic labelling experiment using the wild-type strain BY4741 (lanes 1 and 2) and the *dcs1*Δ strain PTC194 (lane 3). [^{32}P]orthophosphate was added to yeast previously grown for 45 min in phosphate-free medium in the presence (lane 1) or absence (lane 2) of glucose. The lower panel shows western blot analysis of immunoprecipitated Dcs1 proteins. The upper panel shows an autoradiograph of the same gel. (**B**) Dcs1 protein treatment with λ PPase. Lane1, Dcs1 purified from yeast cells at stationary phase and used in lanes 2 and 3. Lane 2, Dcs1 after incubation with λ PPase and phosphatase inhibitor. Lane 3, Dcs1 after incubation with only λ PPase. (**C**) Western blot using anti-Dcs1 antibodies. Late log phase extracts from mutant strains were analysed in the following order: lane 1, MY1 (wild-type strain); lane 2, MY2872 (*rim15*Δ strain); lane 3, MY3297 (*rim15*Δ *yak1*Δ strain); lane 4, MY3273 (*rim15*Δ *yak1*Δ *tpk1-3*Δ strain); lane 5, MY2677 (*msn2*Δ *msn4*Δ strain); lane 6, BY4741 (wild-type strain); lane 7, PTC195 (*dcs1*Δ *dcs2*Δ strain). (**D**) Western blot using anti-Dcs1 antibodies. Late log phase extracts were prepared from PTC194 cells transformed with pRS313-DCS1 (lane 1), pRS313-DCS1-178 (lane 2) and pRS313-DCS1-196 (lane 3). Arrowheads indicate the positions of the phosphorylated form of Dcs1 protein in (A–D).

slower running band seen in Figure 4A (Dcs1) does indeed contain a phosphorylated form of this protein (Figure 5A). Further evidence that the Dcs1 modification is a phosphate group was obtained by treating the modified protein with λ protein phosphatase (λPPase). This treatment yielded only the faster migrating form of Dcs1 (Figure 5B, lane 3), thus confirming that Dcs1 is converted to a phosphorylated protein in response to glucose deprivation.

Partial protein degradation revealed that the appearance of a slower migrating (phosphorylated) form of Dcs1 is eliminated if in the N-terminal 70 amino acids of the protein are removed (data not shown). We therefore examined this N-terminal region of the Dcs1 protein sequence for the presence of potential phosphorylation sites, identifying S60 and T66. We then tested appropriate kinase mutants for their effects on Dcs1 phosphorylation (Figure 5C). Comparison of lanes 1, 2 and 3 in Figure 5C indicates that Yak1 plays a major role in the phosphorylation of Dcs1, since in its absence >90% of the upper band intensity is lost. As shown in Figure 5D, replacement of wild-type Dcs1 by the T66A form in a wild-type strain also eliminated the phosphoprotein. In further experiments, we established that the T66A mutation does not cause either of the compromised stress-response phenotypes typical of *dcs1*Δ or *dcs1*Δ*dcs2*Δ (data not shown). The retention of a small amount of the slower running Dcs1 band in the absence of Yak1 is likely to be attributable to a low level of phosphorylation of Dcs1 at other sites (catalysed by other kinases).

Both *DCS* genes are regulatory targets of the cAMP-protein kinase A pathway

Both a previous report (33) and the data presented in Figures 1 and 4 indicate that *DCS2* expression is controlled by the cAMP-PKA pathway [for review, see (14)]. We also observed that *DCS1* gene expression follows a similar pattern to that of *DCS2* (Figure 4A and B). In order to investigate whether *DCS1* gene expression is responsive to the cAMP-PKA pathway, we compared Dcs1 levels in strains containing single or combined disruptions of *RIM15* and *YAK1* (which encode protein kinases involved in growth regulation), *TPK1-3* (which encode PKA catalytic subunits) and *MSN2MSN4* (which encode stress-inducible transcription activators that are negatively controlled by PKA). We found that Dcs1 abundance was drastically decreased in *msn2msn4* cells (Figure 5C, lane 5), while it was much increased in *rim15yak1tpk1tpk2tpk3* compared with the *rim15yak1* strain (Figure 5C, compare lanes 4 and 3). Moreover, the strain lacking the Rim15 protein kinase, which has been described as a stimulator of STRE-controlled genes (14), showed a reduced level of Dcs1 protein (Figure 5C, lane 2). Taken together, these results indicate that expression of *DCS1* is also at least partially responsive to the cAMP-PKA pathway.

Is Dcs1 a modulator of trehalase activity?

We next investigated the possibility that Dcs1 might influence the stress response by directly modulating Nth1 activity. If this were the case, we would expect purified Dcs1 protein to be capable of suppressing the enhanced Nth1 activity observed in extracts from a *dcs1*Δ strain (see Figure 4D). Neither recombinant Dcs1 purified from *E.coli* nor phosphorylated or non-phosphorylated forms of Dcs1 isolated from *S.cerevisiae* showed any significant ability to down-regulate trehalase activity (Figure 6). This indicates that Dcs1 itself does not impose post-translational regulation on Nth1.

Functional overlap between Dcs1 and eIF4E

Since Dcs1 and the translation initiation factor eIF4E both bind to the mRNA cap, we wondered whether there is any functional interaction between the two *in vivo*. This is relevant to the impact that changes in the level of 5′ m^{7}G-capped mRNA fragments may have on the cell. From previous work (40), we know that eIF4E is in considerable excess over eIF4G, the other core component of the cap-binding complex eIF4F, in *S.cerevisiae*. This means that there is a considerable population of eIF4E potentially available in the cell that might be involved in activities other than translation. We decided to explore the possible relationship between the two proteins using a strain (YTH3) in which the eIF4E gene (*CDC33*) has been placed under the control of a promoter that can be regulated via a tetracycline-responsive operator (40). This enabled us to vary the amount of eIF4E in the cell by adding doxycycline to different final concentrations (Figure 7). By means of genetic mating followed by sporulation, we generated a YTH3 *dcs1*Δ strain that could be compared with the YTH3 isogenic parent. In the absence of functional Dcs1, we observed that yeast became highly

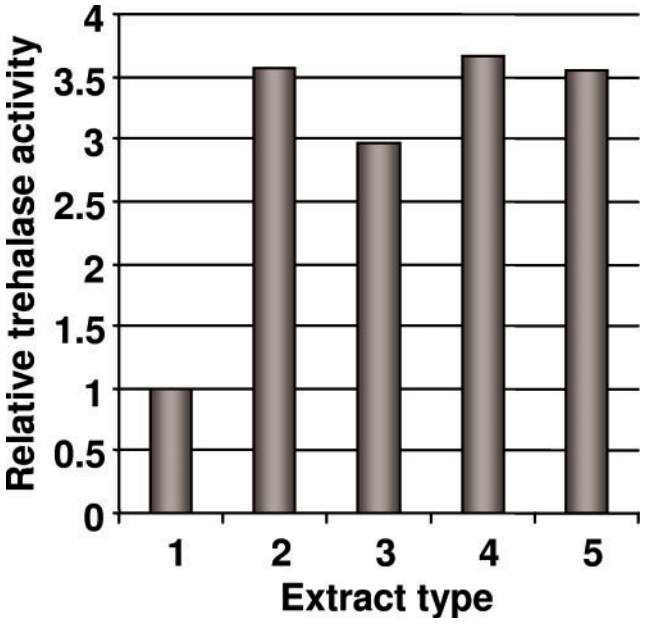

Figure 6. Effect of Dcs1 protein on Nth1 activity in cell extracts. Cell extracts were pre-incubated at 30°C for 30 min with or without additional proteins, and trehalase activity was estimated. Lanes were loaded as follows: lane 1, BY4741 (wild-type strain); lane 2, PTC194 (*dcs1*Δ strain); lane 3, mixture of PTC194 and PTC195 (*dcs1*Δ *dcs1*Δ strain); lane 4, PTC194 with 1 μM of Dcs1 protein purified from the *E.coli*; lane 5, PTC194 with 1 μM of phosphorylated/unphosphorylated form of $Dcs1^{CBD}$ protein and 1 μM of Dcs2 protein purified from the *S.cerevisiae*. The increase in trehalase activity is expressed as a ratio to the activity of BY4741 cells (set at 1).

sensitive to reductions in the level of intracellular eIF4E. Indeed, at high doxycycline concentrations, the combination of the P_{tet}*CDC33* and *dcs1*Δ alleles was synthetic lethal. In control experiments, we observed that the strain bearing *dcs1*Δ alone was not affected by doxycycline at either concentration (data not shown).

CONCLUSIONS

The results described in this paper indicate that the Dcs proteins influence the ability of yeast to respond to both nutrient deficiency and to nutrient availability. Most striking is the observation of two distinct modes of *DCS* gene regulation as glucose becomes scarce during the diauxic shift. Both *DCS2* and *DCS1* are subject to STRE-dependent transcriptional up-regulation, while the Dcs1 protein is also subject to phosphorylation. The transcriptional regulation involves the cAMP-PKA pathway. Since we have observed that Dcs1 and Dcs2 can form a heterodimer, the induction of Dcs2 synthesis under conditions of glucose deprivation is likely to lead to the replacement of much of the homodimeric Dcs1 population by the Dcs1–Dcs2 heterodimer. We note that Dcs2 modulates the impact of Dcs1 on the nutrient stress response, whilst itself not being able to substitute for Dcs1. We have therefore identified a function for Dcs2, which was previously found not to participate in decapping (8).

Transcription of the *NTH1* gene, which also features STREs in its promoter region, increases in response to diauxie (41,42). Yet Nth1 activity decreases under the same conditions (37),

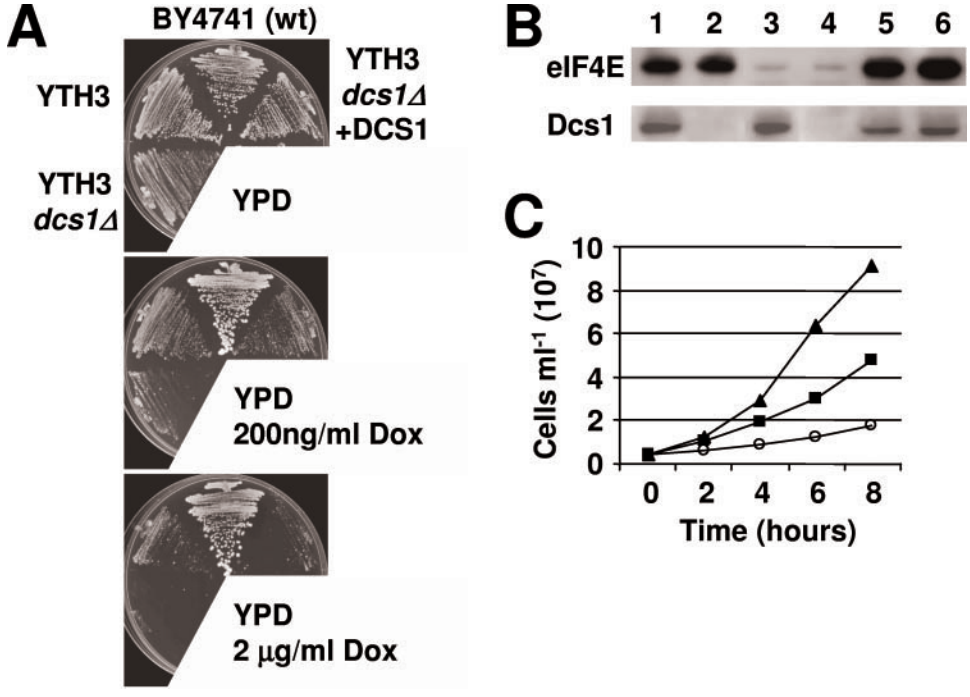

Figure 7. Suppressed *CDC33* expression is synthetic lethal with *dcs1*Δ. (**A**) BY4741 (wt), YTH3 (tetO7 promoter-controlled *CDC33* strain), YTH3 *dcs1*Δ (YTH3 with *dcs1*Δ mutation) and YTH3 *dcs1*Δ+DCS1 (YTH3 *dcs1*Δ transformed with pRS313-DCS1 plasmid) strains were streaked out on YPD medium without (top plate), or with 200 ng (middle plate) or 2 mg (bottom plate) doxycycline per millilitre of medium. Plates were incubated at 30°C for 3 days. (**B**) Western blot using antibodies against eIF4E and Dcs1 proteins. The extracts were prepared from the cells at mid log phase. YTH3 (lanes 1 and 3) and YTH3*dcs1*Δ (lanes 2 and 4) were grown in the absence (lanes 1 and 2) or presence (lanes 3 and 4) of 200 ng/ml of doxycycline. Corresponding controls of extracts prepared from the wild-type strain BY4741 are shown in lanes 5 and 6. (**C**) Cell number as a function of time in yeast cultures incubated in YPD medium at 30°C in the presence of 200 ng/ml of doxycycline. The strains were BY4741 (triangles), YTH3 (squares) and YTH3*dcs1*Δ (circles). Each data point represents the mean of three independent experiments.

and it has been proposed that this is attributable to Dcs1-dependent inhibition at the protein level (39). In this context it is notable that Thevelein previously suggested that cAMP-dependent PKA-mediated phosphorylation is involved in the regulation of Nth1 activity (43), leading to the proposal that phosphorylation might be used to modulate an interaction between Dcs1 and Nth1 (39). However, we have found no evidence of direct regulation of trehalase activity by Dcs1, irrespective of the phosphorylation state of the latter protein. An alternative interpretation is that increased levels of m^7G-oligoribonucleotides, as present in *dcs1* mutants, serve to trigger a stress response. Like other known stressors (37,44), they may act to induce increased Nth1 activity. The mechanism by which the cell senses enhanced levels of m^7G-oligoribonucleotides is unclear, but one possibility is that the response is coupled to interactions of these competitive inhibitors with the translational apparatus (Figure 8). The observation that expression of a P_{NTH1}*lacZ* fusion is almost three times higher in a *dcs1*Δ strain than that in an isogenic wild-type strain (39) indicates that this increased activity is at least partly due to transcriptional control, although the involvement of some element of post-transcriptional control cannot be ruled out.

The observation that reduced levels of the cap-binding protein eIF4E cause strong synthetic phenotypes in a *dcs1*Δ mutant shows that a normal cellular content of eIF4E partially complements Dcs1 deficiency. The most likely explanation of this is that eIF4E can 'buffer' to some extent the effects of an excess of 5′ m^7G-oligoribonucleotides on cellular processes (such as translation initiation). This suggests a model in which the inhibitory potential of m^7G-oligoribonucleotides is modulated by the activity of (free) eIF4E (Figure 8). There seems to be an interplay between Dcs protein activity and the nutrient stress response. In the absence of pyrophosphatase activity capable of hydrolysing m^7G-oligoribonucleotides, the prolonged longevity of these species causes an additionally stressed state under conditions of glucose depletion. This, in

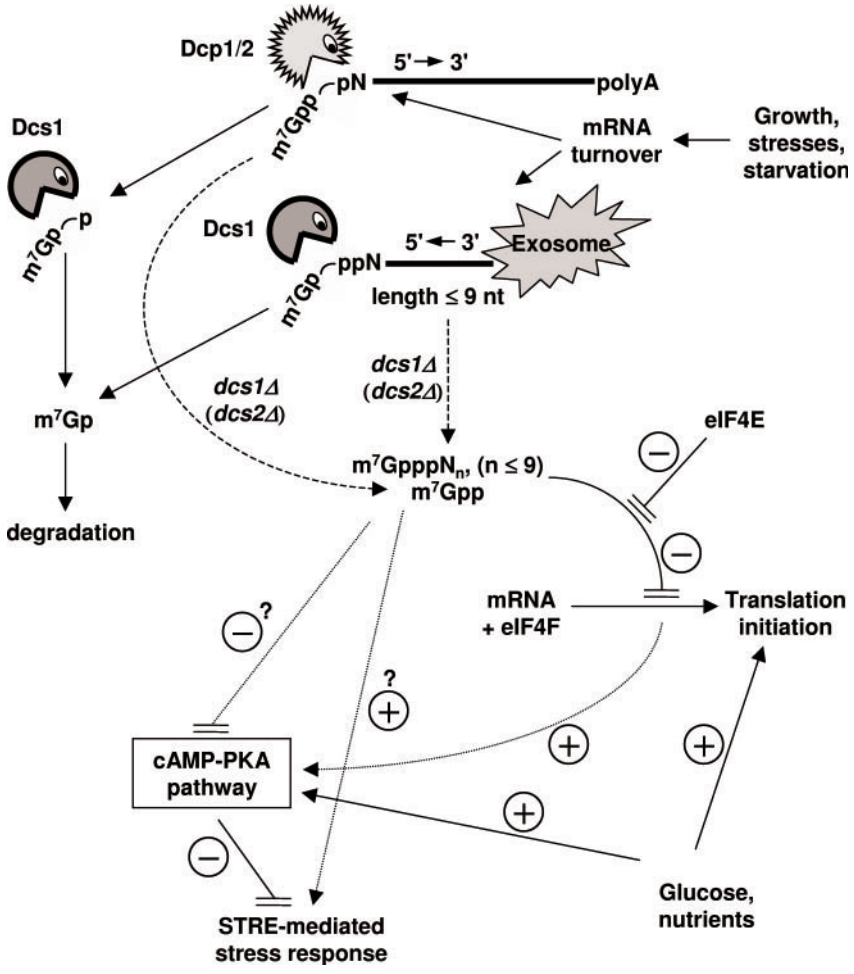

Figure 8. A testable model for the modulating role of Dcs1 in the yeast stress response. Increases in yeast growth rate, or stress conditions, can accelerate mRNA turnover, thus increasing the rate of generation of mRNA turnover products, including m^7G-oligoribonucleotides, m^7GDP and other m^7G-derivatives. In the 5′→3′ pathway, decapping of deadenylated but capped mRNA yields m^7GDP, which is a substrate of Dcs1. In the 3′→5′ pathway, m^7G-oligoribonucleotides are the final products of exosome-catalysed degradation. Where there is a reduction in the activity of Dcs1 (and more markedly where Dcs2 activity is also reduced), m^7G-oligoribonucleotides and m^7GDP levels increase and compete with capped mRNA for eIF4F and thereby inhibit translation initiation. In our experiments, we studied the extreme case where *DCS1* and/or *DCS2* were disrupted. Due to this inhibition, or possibly via an alternative stimulatory route, cAMP-PKA-mediated activation of STRE-promoters occurs, inducing a stressed state. Dashed arrows represent pathways that generate strong inhibitors of translation. Dotted arrows indicate potential stimulatory routes for STRE-dependent transcriptional activation, with the cAMP-PKA pathway providing one such route. In the latter case, inhibition of cAMP-PKA activity has to be repressed in order for transcription to be stimulated.

turn, may induce enhanced trehalase activity in the stationary phase and compromise the cellular response to nutrient stress. It is not known whether the levels of m^7G-oligoribonucleotides can influence STRE-mediated regulation of stress genes via alternative routes (Figure 8). In conclusion, the Dcs1 and Dcs2 activities in yeast show the novel property of being able to modulate the nutrient stress response and this organism's adaptation to nutrient availability. Future work will need to elucidate the relationship between m^7G-oligoribonucleotide turnover and parts of these responses, including the control of trehalase activity.

Finally, other organisms possess further members of the HIT motif superfamily which are closely related to *S.cerevisiae* Dcs1. Do these proteins constitute a subgroup whose members all manifest the same functional properties? Certainly the human DcpS protein manifests similar decapping properties to *S.cerevisiae* Dcs1 (9), although we do not yet know whether it too is required for the nutrient stress response. On the other hand, the cellular function of *S.pombe* Nhm1, much of which is nuclear (10), remains unclear. We also note that despite being very similar in structure to Dcs1, *S.cerevisiae* Dcs2 is clearly functionally distinct. There may therefore be significant diversity of function within the family of Dcs-like HIT proteins.

ACKNOWLEDGEMENTS

We thank Dr M. A. Collart (Department Biochimie Medicale, Geneva, Switzerland) for donating some yeast strains, and the BBSRC (UK) and the Wellcome Trust (UK) for financial support.

REFERENCES

1. McCarthy,J.E.G. (1998) Post-Transcriptional control of gene expression in yeast. *Microbiol. Mol. Biol. Rev*., **62**, 1492–1553.
2. Wang,Z. and Kiledjian,M. (2001) Functional link between the mammalian exosome and mRNA decapping. *Cell*, **107**, 751–762.
3. van Hoof,A. and Parker,R. (2002) Messenger RNA degradation: beginning at the end. *Curr. Biol*., **12**, R285–R287.
4. Steiger,M.A. and Parker,R. (2002) Analyzing mRNA decay in *Saccharomyces cerevisiae*. *Methods Enzymol*., **351**, 648–660
5. Larimer,F.W. and Stevens,A. (1990) Disruption of the gene *XRN1*, coding for a 5′→3′ exoribonuclease, restricts yeast cell growth. *Gene*, **95**, 85–90.
6. LeGrandeur,T.E. and Parker,R. (1998) Isolation and characterisation of Dcp1p, the yeast mRNA decapping enzyme. *EMBO J*., **17**, 1487–1496.
7. Decker,C.J. and Parker,R. (2002) mRNA decay enzymes: Decappers conserved between yeast and mammals. *Proc. Natl Acad. Sci. USA*, **99**, 12512–12514
8. Nuss,D.L. and Furuichi,Y. (1977) Characterization of the m7G(5′)pppN-pyrophosphatase activity from HeLa cells. *J. Biol. Chem*., **252**, 2815–2821.
9. Liu,H., Rodgers,N.D., Jiao,X. and Kiledjian,M. (2002). The scavenger mRNA decapping enzyme DcpS is a member of the HIT family of pyrophosphatases. *EMBO J*., **21**, 4699–4708.
10. Salehi,Z., Geffers,L., Vilela,C., Birkenhäger,R., Ptushkina,M., Berthelot,K., Ferro,M., Gaskell,S., Hagan,I., Stapley,B. and McCarthy,J.E.G. (2002) A nuclear protein in *Schizosaccharomyces pombe* with homology to the human tumour suppressor Fhit has decapping activity. *Mol. Microbiol*., **46**, 49–62.
11. Boy-Marcotte,E., Perrot,M., Bussereau,F., Boucherie,H. and Jacquet,M.(1998) Msn2p and Msn4p control a large number of genes induced at the diauxic transition, which are repressed by cyclic AMP in *Saccharomyces cerevisiae*. *J. Bacteriol*., **180**, 1044–1052.
12. Martinez-Pastor,M.T., Marchler,G., Schuller,C., Marchler-Bauer,A., Ruis,H. and Estruch,F. (1996) The *Saccharomyces cerevisiae* zinc finger proteins Msn2p and Msn4p are required for transcriptional induction through the stress response element (STRE). *EMBO J*., **15**, 2227–2235.
13. Gorner,W., Durchschlag,E., Martinez-Pastor,M.T., Estruch,F., Ammerer,G., Hamilton,B., Ruis,H. and Schuller,C. (1998) Nuclear localization of the C2H2 zinc finger protein Msn2p is regulated by stress and protein kinase A activity. *Genes Dev*., **12**, 586–597.
14. Thevelein,J.M. and de Winde,J.H. (1999) Novel sensing mechanisms and targets for the cAMP-protein kinase A pathway in the yeast *Saccharomyces cerevisiae*. *Mol. Microbiol*., **33**, 904–918.
15. Lenssen,E., Oberholzer,U., Labarre,J., De Virgilio,C. and Collart,M.A. (2002) *Saccharomyces cerevisiae* Ccr4-not complex contributes to the control of Msn2p-dependent transcription by the Ras/cAMP pathway. *Mol. Microbiol*., **43**, 1023–1037.
16. Moriya,H., Shimizu-Yoshida,Y., Omori,A., Iwashita,S., Katoh,M. and Sakai,A. (2001) Yak1p, a DYRK family kinase, translocates to the nucleus and phosphorylates yeast Pop2p in response to a glucose signal. *Genes Dev*., **15**, 1217–1228.
17. Crespo,J.L. and Hall,M.N. (2002) Elucidating TOR signaling and rapamycin action: lessons from *Saccharomyces cerevisiae*. *Microbiol. Mol. Biol. Rev*., **66**, 579–591.
18. Hohmann,S. (2002) Osmotic stress signaling and osmoadaptation in yeasts. *Microbiol. Mol. Biol. Rev*., **66**, 300–372.
19. Mager,W.H. and Siderius,M. (2002) Novel insights into the osmotic stress response of yeast. *FEMS Yeast Res*., **2**, 251–257.
20. Schmelzle,T., Beck,T., Martin,D.E. and Hall,M.N. (2004) Activation of the RAS/cyclic AMP pathway suppresses a TOR deficiency in yeast. *Mol. Cell. Biol*., **24**, 338–351.
21. Sikorski,R.S., Hieter,P. (1989) A system of shuttle vectors and yeast host strains designed for efficient manipulation of DNA in *Saccharomyces cerevisiae*. *Genetics*, **122**, 19–27.
22. Kuipers,O.P., Boot,H.J. and de Vos,W.M. (1991) Improved site-directed mutagenesis method using PCR. *Nucleic Acids Res*., **19**, 4558.
23. Oliveira,C.C., van den Heuvel,J.J. and McCarthy,J.E. (1993) Inhibition of translational initiation in *Saccharomyces cerevisiae* by secondary structure: the roles of the stability and position of stem-loops in the mRNA leader. *Mol. Microbiol*., **9**, 521–532.
24. Rigaut,G., Schevchenko,A., Rutz,B., Wilm,M., Mann,M. and Séraphin,B. (1999) A generic protein purification method for protein complex characterization and proteome exploration. *Nature Biotechnol*., **17**, 1030–1032.
25. Kuhn,K.M., DeRisi,J.L., Brown,P.O. and Sarnow,P. (2001) Global and specific translational regulation in the genomic response of *Saccharomyces cerevisiae* to a rapid transfer from a fermentable to a nonfermentable carbon source. *Mol. Cell. Biol*., **21**, 916–927.
26. App,H. and Holzer,H. (1989) Purification and characterization of neutral trehalase from the yeast ABYS1 mutant. *J. Biol. Chem*., **264**, 17583–17588.
27. Warner,J.R. (1991) Labeling of RNA and phosphoproteins in *Saccharomyces cerevisiae*. *Methods Enzymol*., **194**, 423–428.
28. Marchler,G., Schuller,C., Adam,G. and Ruis,H. (1993) A *Saccharomyces cerevisiae* UAS element controlled by protein kinase A activates transcription in response to a variety of stress conditions. *EMBO J*., **12**, 1997–2003.
29. Nuss,D.L., Altschuler,R.E. and Peterson,A.J. (1982) Purification and characterization of the m^7G(5′)pppN-pyrophosphatase from human placenta. *J. Biol. Chem*., **257**, 6224–6230.
30. Baudin,A., Ozier-Kalogeropoulos,O., Denouel,A., Lacroute,F. and Cullin,C. (1993) A simple and efficient method for direct gene deletion in *Saccharomyces cerevisiae*. *Nucleic Acids Res*., **21**, 3329–3330.
31. Gancedo,J.M. (1998) Yeast carbon catabolite repression. *Microbiol. Mol. Biol. Rev*., **62**, 334–361.
32. Gasch,A.P., Spellman,P.T., Kao,C.M., Carmel-Harel,O., Eisen,M.B., Storz,G., Botstein,D. and Brown,P.O. (2000). Genomic expression programs in the response of yeast cells to environmental changes. *Mol. Biol. Cell*, **11**, 4241–4257.
33. Tadi,D., Hasan,R.N., Bussereau,F., Boy-Marcotte,E. and Jacquet,M. (1999) Selection of genes repressed by cAMP that are induced by nutritional limitation in *Saccharomyces cerevisiae*. *Yeast*, **15**, 1733–1745.
34. Uetz,P., Giot,L., Cagney,G., Mansfield,T.A., Judson,R.S., Knight,J.R., Lock Shon,D., Narayan,V., Srinivasan,M. Pochart,P. *et al*. (2000) A comprehensive analysis of protein–protein interactions in *Saccharomyces cerevisiae*. *Nature*, **403**, 623–627.

35. Ito,T., Chiba,T., Ozawa,R., Yoshida,M., Hattori,M. and Sakaki,Y. (2001) A comprehensive two-hybrid analysis to explore the yeast protein interactome. *Proc. Natl Acad. Sci. USA*, **98**, 4569–4574.
36. Nwaka,S. and Holzer,H. (1998) Molecular biology of trehalose and the trehalases in the yeast *Saccharomyces cerevisiae*. In Moldave, K. (ed.), *Progress in Nucleic Acid Research and Molecular Biology*. Academic Press, San Diego, CA, Vol. 58, pp. 197–237.
37. Zähringer,H., Thevelein,J.M. and Nwaka,S. (2000). Induction of neutral trehalase Nth1 by heat and osmotic stress is controlled by STRE elements and Msn2/Msn4 transcription factors: variations of PKA effect during stress and growth. *Mol. Microbiol.*, **35**, 397–406.
38. Piper,P.W. (1998) Differential role of Hsps and trehalose in stress tolerance. *Trends Microbiol.*, **6**, 43–44.
39. De Mesquita,J.F., Panek,A.D. and de Araujo,P.S. (2003). *In silico* and *in vivo* analysis reveal a novel gene in *Saccharomyces cerevisiae* trehalose metabolism. *BMC Genomics*, **4**, 45.
40. von der Haar,T. and McCarthy,J.E.G. (2002) Intracellular translation initiation factor levels in *Saccharomyces cerevisiae* and their role in cap-complex function. *Mol. Microbiol.*, **46**, 531–544.
41. DeRisi,J., Iyer,V.R. and Brown,P.O. (1997) Exploring the metabolic and genetic control of gene expression on a genomic scale. *Science*, **278**, 680–686.
42. Zähringer,H., Holzer,H. and Nwaka,S. (1998) Stability of neutral trehalase during heat stress in *Saccharomyces cerevisiae* is dependent on the activity of the catalytic subunits of cAMP-dependent protein kinase, Tpk1 and Tpk2. *Eur. J. Biochem.*, **255**, 544–551.
43. Thevelein,J.M. (1984) Regulation of trehalose mobilization in fungi. *Microbiol. Rev.*, **48**, 42–59.
44. Zähringer,H., Burgert,M., Holzer,H. and Nwaka,S. (1997) Neutral trehalase Nth1p of *Saccharomyces cerevisiae* encoded by the *NTH1* gene is a multiple stress responsive protein. *FEBS Lett.*, **412**, 615–620.